HHS Public Access

Author manuscript

Transplantation. Author manuscript; available in PMC 2016 April 01.

Published in final edited form as:

Transplantation. 2015 April ; 99(4): 668–677. doi:10.1097/TP.0000000000000561.

VEGF-C/VEGFR-3 Signaling Regulates Chemokine Gradients and Lymphocyte Migration from Tissues to Lymphatics

Daiki Iwami[1], **C. Colin Brinkman**[1], and **Jonathan S. Bromberg**[1,2,3]

Daiki Iwami: iwamidaiki@ybb.ne.jp; C. Colin Brinkman: colin.brinkman@gmail.com

[1]Center for Vascular and Inflammatory Diseases, University of Maryland School of Medicine, Baltimore, MD, 21201, USA

[2]Department of Microbiology and Immunology, University of Maryland School of Medicine, Baltimore, MD, 21201, USA

[3]Department of Surgery, University of Maryland School of Medicine, Baltimore, MD, 21201, USA

Abstract

Background—Circulation of leukocytes via blood, tissue and lymph is integral to adaptive immunity. Afferent lymphatics form CCL21 gradients to guide DC and T cells to lymphatics and then to draining lymph nodes (dLN). VEGF-C and VEGFR-3 are the major lymphatic growth factor and receptor. We hypothesized these molecules also regulate chemokine gradients and lymphatic migration.

Methods—$CD4^+$ T cells were injected into the foot pad or ear pinnae, and migration to afferent lymphatics and dLN quantified by flow cytometry or whole mount immunohistochemistry. VEGFR-3 or its signaling or downstream actions were modified with blocking mAbs or other reagents.

Results—Anti-VEGFR-3 prevented migration of $CD4^+$ T cells into lymphatic lumen and significantly decreased the number that migrated to dLN. Anti-VEGFR-3 abolished CCL21 gradients around lymphatics, although CCL21 production was not inhibited. Heparan sulfate (HS), critical to establish CCL21 gradients, was down-regulated around lymphatics by anti-VEGFR-3 and this was dependent on heparanase-mediated degradation. Moreover, a PI3Kα inhibitor disrupted HS and CCL21 gradients,while a PI3K activator prevented the effects of anti-VEGFR-3. During contact hypersensitivity, VEGFR-3, CCL21, and HS expression were all attenuated, and anti-heparanase or PI3K activator reversed these effects.

Conclusions—VEGF-C/VEGFR-3 signaling through PI3Kα regulates the activity of heparanase, which modifies HS and CCL21 gradients around lymphatics. The functional and physical linkages of these molecules regulate lymphatic migration from tissues to dLN. These represent new therapeutic targets to influence immunity and inflammation.

Correspondence Address: Jonathan S. Bromberg, Department of Surgery, University of Maryland School of Medicine, 29 S. Greene Street, Suite 200, Baltimore, MD 20201, jbromberg@smail.umaryland.edu, Phone: 410 328 0008, Fax: 410 328 6343.

Disclosure: The authors declare no conflict of interest.

Authorship Contribution: D.I. designed the research, performed experiments, analyzed results and wrote the manuscript.
C.C.B. designed the research, and provided advice for experiments.
J.S.B. designed the research, contributed materials, provided advice, and wrote the manuscript.

Introduction

Immune surveillance requires continuous recruitment of lymphocytes from blood through high endothelial venules (HEV) into lymph nodes (LN) where they encounter dendritic cells (DC) to initiate adaptive immunity (1). In addition to HEV-mediated migration naïve T cells migrate from tissues to the draining LN (dLN) through afferent lymphatics as a normal migratory pathway (2).

Previously, it had been assumed that lymphocytes passively and randomly enter afferent lymphatics (3). This changed after the identification of CCR7, highly expressed on naïve T cells and mature DC, which regulates entry into afferent lymphatics (4,5). The chemokine CCL21 is essential for attracting T cells and DC to LN (6). The importance of CCL21-CCR7 interaction was demonstrated in *Ccr7-/-* mice and *plt/plt* mice that lack *Ccl19* and *Ccl21* expression in lymphoid organs, resulting in severe defects in T cells and DC migration (7,8). However, the underlying molecular mechanisms that affect leukocytic migration during steady and inflammatory states are incompletely understood.

Heparan sulfate (HS) is a component of heparan sulfate proteoglycan, ubiquitously expressed in extracellular matrices (ECM) and on endothelial cell (EC) surfaces (9). HS functions as a physical barrier to leukocyte extravasation (10), and immobilizes chemokines and establishes chemokine gradients in the interstitium (9). CCL21 has a C-terminal domain which binds to glycosaminoglycans (11,12) leading to its immobilization. Impairment of HS structure or expression results in reduction of the gradient, leading to inappropriate positioning and migration of leukocytes (13,14). Topical administration of heparanase (HPSE) degrades HS, disrupts the tissue chemokine gradient, and prevents CCL21-induced migration of DC toward lymphatics (15). In mice lacking HS-synthetic enzyme exostoses-1, CCL21 presentation but not transcription is diminished, causing a marked decrease in lymphocyte recruitment to LN (13,16).

HPSE is the only known mammalian endoglycosidase which cleaves HS side chains of heparan sulfate proteoglycan facilitating cell invasion (17,18). Furthermore, HPSE activity results in release of HS-bound molecules (19). HPSE is expressed by leukocytes (19) and activated EC (20), and is up-regulated by various inflammatory stimuli (18,21) and hypoxia (22). In hypoxia-induced retinal diseases, HPSE is increased and associated with vascular endothelial growth factor (VEGF) expression in human retinal EC (22), suggesting a relationship among chemokines, HS, HPSE, endothelial growth and immune responses.

VEGFR-3 is expressed primarily on the surface of LEC (23). VEGF-C is the most potent promoter of lymphangiogenesis through VEGFR-2 and VEGFR-3 (24–26). VEGF-C is constitutively expressed in normal epidermis (27) and keratinocyes and fibroblasts are the principal producers (28,29). Anti-VEGFR-3 mAb suppresses CCL21 production in chronically rejecting cardiac allografts, leading to reduced infiltrating cells (30). Blockade of VEGFR-3 suppresses DC trafficking to dLN and corneal allograft rejection (31), and inhibits islet allograft rejection and autoimmune insulitis (32,33). VEGF-C also increases CCL21 secretion by LEC (34). However, the physiological role of VEGF-C/VEGFR-3

signaling for homeostatic migration of leukocytes and the molecular mechanisms of how VEGFR-3 signaling regulates LEC function are not known.

We show here that anti-VEGFR-3 mAb suppressed entry of naïve $CD4^+$ T cells from tissue into afferent lymphatics by disrupting the CCL21 gradient around LEC. The disruption was accompanied by HPSE-dependent degradation of the HS scaffold surrounding lymphatics to which CCL21 was bound. During an acute inflammatory response, VEGFR-3 expression was down-modulated, resulting in a similar series of changes to HPSE, HS, and CCL21. These data demonstrated that VEGF-C/VEGFR-3 signaling regulates LEC functions and lymphocyte migration in the homeostatic and inflammatory states.

Materials and Methods

Mice

C57BL/6 mice 8–10 weeks old purchased from The Jackson Laboratory. Mice were housed in microisolator cages in a pathogen–free facility. Experiments used age- and sex-matched mice in accordance with protocols approved by the Institutional Animal Care and Use Committee.

Reagents

Neutralizing monoclonal rat anti-VEGFR-3 (m4F-31C1) and control rat IgG2a antibody (2A3) were gifts from Dr. Pytowski (ImClone Systems, Eli Lilly and Company) (35). Neutralizing polyclonal rabbit anti-HPSE antibody (bs-1541R) was purchased from Bioss (Woburn, MA), which inhibits HPSE activity by binding its active site. Antibodies for flow cytometry and IHC are listed in the SDC Table1 and Table2. Human recombinant VEGF-C was purchased from R&D Systems. Phosphoinositide 3-kinase (PI3K) α-specific inhibitor (PIK2) and pan-PI3K stimulator (740Y-P) were purchased from Echelon Biosciences Inc. and from Cayman, respectively.

Cell preparation

Mice were euthanized, and spleens and LN dissociated into single-cell suspensions. $CD4^+$ T Cells were enriched with EasySep $CD4^+$ T cell Enrichment Kit (STEMCELL Technologies Inc.). Enriched populations routinely were 90-95% $CD4^+$ live leukocytes.

Adoptive transfers

$CD4^+$ T cell suspensions were labeled with 1 μM CFSE 10 minutes at 37°C. Three $\times 10^6$ CFSE-labeled $CD4^+$ T cells in 20μl PBS were injected into the foot pad. Alternatively, 1×10^6 cells in 20μl PBS were injected into ear pinna to assess interstitial migration. Indicated amounts of anti-VEGFR-3 or control mAb were added to cell suspensions.

Preparation of single-cell suspension from ear pinna

Control mAb (2A3, 7μg/ear) or anti-VEGFR-3 mAb (m4F-31C1, 7μg/ear) treated ear pinnae were digested with Collagenase D (0.4 mg/ml, 30 minutes, 37 °C). Cell suspensions were passed twice through a cell strainer, washed, and resuspended in FACS buffer.

LN LEC sorting

LN LEC were isolated as previously described (36) by using a MACS magnetic column and flow sorting (FACSAria, BD Biosciences).

Contact hypersensitivity

25 μl 0.5% (v/v) 2,4-dinitrofluorobenzene (DNFB; Wako) in acetone/olive oil (4:1) was applied onto shaved mouse abdominal skin on day 0. On day 5, the right ear was treated with 20 μl 0.2% DNFB (10 μl on each side), and the left ear was treated with vehicle. Ears were injected with neutralizing anti-HPSE Ab (1μg/20μl PBS/ear), pan-PI3K stimulator, 740Y-P (10μg/20μl PBS/ear), or PBS (20μl/ear) 36 hours after DNFB. Ear thickness was measured with Digimatic calipers (Marathon Watch Company) before and 48 h after challenge. Mice were euthanized 48 hours after challenge, ears fixed with 4% paraformaldehyde (PFA) in PBS and used for immunohistochemistry.

Immunohistochemistry Staining

Five μm cryosections of tissue were fixed with ice-cold acetone. After incubation with PBS/0.5%BSA/0.3%Triton and blocking buffer (PBS with 5% donkey serum), sections were incubated with primary Ab in PBS for 1 hour, followed by secondary Ab in PBS for 1 hour at room temperature. In some samples, immunofluorescence was amplified with tyramide signal amplification (TSA, PerkinElmer).

For whole mount IHC, ear skin sheets separated, fixed with 4% PFA, incubated with PBS/0.5%BSA/0.3%Triton for 10 min, blocked with blocking buffer for 1 hour, incubated with primary Ab, washed with PBS/0.5%BSA/0.3%Triton, incubated with secondary Ab. All samples were mounted with ProLong Gold antifade reagent (Life Technologies). Fluorescent images were collected with a Nikon Eclipse E800 (Nikon Co.) equipped with a digital CCD camera RETIGA EXi FAST 1394 (Qimaging).

Computer-assisted morphometric analyses

Quantitative analyses of CCL21 and HS in tissue lymphatics were performed with Volocity 3D Image Analysis Software (PerkinElmer). LYVE-1^+ lymphatics were traced and indicated as ROI (also shown in Fig.2B), and number of CCL21 aggregates, staining intensity of CCL21 and HS, and %CCL21- and %HS-positive area in lymphatics were calculated.

Flow cytometry

Washes and Ab dilutions were performed in PBS/1% BSA at 4°C. Purified anti-mouse CD16/32 (BD Biosciences) was used to block Fc receptors. Surface staining was performed for 30 min with the corresponding cocktail of fluorescently labeled Ab. After surface staining, cells were fixed and intracellularly stained for Foxp3 using Foxp3 Staining Buffer Set (eBioscience). Flow cytometric analysis was performed on BD LSRFortessa cell analyzer (BD Biosciences) and analyzed with FlowJo software (Tree Star, Inc.). $CD45^-CD31^+$ cells were gated, and LEC ($CD31^+gp38^+$) and blood endothelial cells (BEC) ($CD31^+gp38^-$) were analyzed for expression of indicated molecules.

qRT-PCR

Total cellular RNA was extracted from the indicated cell populations, transcribed to cDNA and quantified by qRT-PCR as previously described (37). Details and primer sequences can be found in the SDC Materials and Methods.

Statistics

In vitro migration results represent mean values of triplicate samples. *In vivo* migration results represent samples from three mice per experiment. The mean and S.D. for percentage of transferred cells in adoptive transfer and transendothelial migration assays were calculated for each condition. For adoptive transfer and transendothelial migration assays, *P* values were calculated with the unpaired Student's *t*-test or one-way analysis of variance (ANOVA) using the GraphPad Prism Software (version 5, GraphPad Software Inc.).

Results

Anti-VEGFR-3 inhibits tissue to afferent lymphatic and draining LN migration

To assess the effect of VEGFR-3 blockade on homeostatic lymphocyte migration, $CD4^+$ T cells were injected into the foot pad together with local treatment with anti-VEGFR-3 or control mAb. Since $CD4^+$ T cells did not express VEGFR-3 protein (Fig. 1A) or mRNA (Fig. 1B), only LEC in the tissue could be affected by the treatments (gating strategy for LEC and BEC shown in Fig. S1A). Indeed, only LYVE-1^+ lymphatics in whole mount staining (Fig. 1C), and only skin $gp38^+CD31^+$ LEC in flow cytometry (Fig. 1A) expressed VEGFR-3, while $gp38^-CD31^+$ BEC did not. In controls, the proportion of transferred cells in total $CD4^+$ cells in dLN 12 hours after transfer did not change significantly with either 2 or 20 μg of control mAb (0.635 ± 0.38% and 0.705 ± 0.313%, respectively, Fig. 1D). As reported previously (37), the fraction of transferred cells peaked at 12 hours. There were almost no transferred cells (0.002 ± 0.003% of total $CD4^+$ T cells) in non-draining LN. In contrast, the proportion of migrated cells was significantly decreased to 0.215 ± 0.28% with 7μg of anti-VEGFR-3 mAb and even more with 20μg (0.031 ± 0.036%) (Fig. 1D). Thus, anti-VEGFR-3 mAb suppressed migration of naïve $CD4^+$ T cells from peripheral tissues to dLN in a dose-dependent manner, presumably by interfering with function of LEC.

Several mechanisms could explain the reduced migration of T cells after anti-VEGFR-3 mAb treatment: first, impairment of interstitial migration toward afferent lymphatics; second, lack of transmigration across lymphatic endothelium; third, impaired movement within the lymphatics toward dLN; and/or fourth, inability to migrate from the subcapsular sinus (SCS) into the dLN parenchyma.

To determine which step of migration was impaired by anti-VEGFR-3, CFSE-labeled $CD4^+$ T cells were adoptively transferred into ear skin tissues and then whole mount ear pinna immunohistochemistry (IHC) was performed by staining for the LEC-specific marker, LYVE-1. In controls, transferred cells were detected both in the tissues near the lymphatics and inside the lymphatic lumen (Fig. 1E and 1F). However, in the anti-VEGFR-3 group, the $CD4^+$ T cells were relatively more abundant in the tissue (Fig. 1E and 1F) at both 12 (Fig. 1F) and 18 hours (not shown). Administration of hVEGF-C along with $CD4^+$ T cells did not

promote further migration into afferent lymphatics (Fig. 1F), suggesting that baseline tonic VEGR-3 stimulation and migration were already optimized. To assess migration within dLN, distribution of $CD4^+$ T cells in dLN was analyzed in the SCS, medullary sinus (MS), cortical ridge (CR), and T cell zone (TCZ). IHC analysis showed 22.44% of transferred cells located in the SCS or MS and 77.43% in the TCZ or CR, in control dLN at 12 hours (Fig. S1B and S1C). In anti-VEGFR-3 treated mice, migration to dLN was significantly decreased, however, the distribution in LN was not significantly changed (Fig. S1B and S1C). Thus, migration was not affected once T cells accessed the lymphatic lumen. Overall, the results showed that anti-VEGFR-3 inhibited migration from the tissues toward lymphatics and into the lymphatic lumen.

Expression and regulation of VEGF-C in the skin lymphatics

The results suggested that tonic VEGFR-3 signaling was important for homeostatic lymphatic migration. Therefore, VEGFR-3 ligands should be available in the steady state. To test this, skin was assayed by IHC. In naïve ears, VEGF-C, the major ligand for VEGFR-3, was stained in cells near LYVE-1^+ LEC, suggesting that skin-derived VEGF-C constitutively stimulated VEGFR-3 on LEC in the steady state (Fig. S2A). In contrast, VEGF-D, the other ligand for VEGFR-3, was not observed (Fig. S2A). When ears were treated with anti-VEGFR-3, there were no significant changes in VEGF-C expression at 6 hours (Fig. S2A). Thus, anti-VEGFR-3 did not inhibit VEGF-C expression, but rather blocked its ability to stimulate the receptor.

VEGFR-3 regulates the CCL21 gradient

Since CCL21 gradients are critical for migration of naïve $CD4^+$ T cells from peripheral tissues to afferent lymphatics and dLN, the expression pattern of CCL21 was characterized. By whole mount IHC, CCL21 was expressed on LEC (LYVE-1^+CD31^+) but not on BEC (LYVE-1^-CD31^+) in control tissues and had a punctate distribution as reported previously (38) (Fig. 2A). Anti-VEGFR-3 significantly down-regulated the size and intensity, but not the number, of CCL21 aggregates, so that the total amount of CCL21 staining was decreased as early as 6 hours after mAb treatment (Fig.2B and S2B). Disruption of the CCL21 gradient lasted for at least 14 hours and recovered in 24 hours (not shown). These results showed that VEGFR-3 blockade rapidly disrupted the CCL21 gradient around the lymphatics. Administration of VEGF-C did not increase CCL21 expression above baseline (not shown), suggesting that the homeostatic expression of VEGF-C and stimulation of VEGFR-3 were already maximal to establish and maintain the chemokine gradient.

There were at least three possible mechanisms by which anti-VEGFR-3 rapidly disrupted the CCL21 gradient. First, down regulated production of CCL21 in LEC; second, accelerated CCL21 degradation; and third, altered ECM components immobilizing CCL21 around lymphatics, leading to disruption of the CCL21 gradient.

To investigate CCL21 production, skin LEC were isolated from control and anti-VEGFR-3 treated pinnae. Flow cytometry revealed low cell surface CCL21 and high intracellular CCL21 expression (Fig S2C). This pattern and degree of expression did not change after anti-VEGFR-3 treatment (Fig S2C). In contrast, IHC of anti-VEGFR-3 treated pinnae

showed a significant reduction in CCL21 compared to the control (Fig. 2B and S2B). CCL21 is expressed on the abluminal side of LEC where it is bound to ECM (39). These data suggested that anti-VEGFR-3 did not inhibit CCL21 production, but increased its extracellular degradation and/or dispersion.

VEGFR-3 regulates heparan sulfate expression

HS is widely distributed in tissues and is critical for immobilization of chemokines to physically establish gradients. Indeed, CCL21 has a HS-binding C-terminal domain which facilitates its immobilization to ECM (40). To assess the last possibility raised above, we performed whole mount IHC for HS expression. The antibody against HS (10E4) detects intact but not digested fragments of HS (13). HS was expressed in the tissues surrounding lymphatics and blood vessels (Fig. 3A). In 4 separate experiments anti-VEGFR-3 treatment inhibited HS expression between at least 6 to 20 hours (Fig. 3A and 3B); and HS expression recovered between 24 to 48 hours (not shown). These results showed that down-regulation or degradation of HS was coincident with the disruption of CCL21 gradients after anti-VEGFR-3 treatment. Taken together, anti-VEGFR-3 mAb disrupted the HS scaffold around lymphatics responsible for establishing CCL21 gradients. Administration of VEGF-C into naive ears did not increase HS expression above baseline (not shown), suggesting that VEGFR-3 stimulated by homeostatic VEGF-C was already maximal to establish and maintain the HS scaffold.

VEGFR-3 regulates heparanase activity

Since VEGF down-regulates expression of HPSE in BEC (41), we determined if LEC express HPSE, and if the effects of anti-VEGFR-3 on HS/CCL21 expression were due to HPSE activity. Flow cytometry and IHC showed that skin LEC expressed HPSE (Fig. 4A and 4B). HPSE was also weakly expressed by other cells, likely BEC (not shown) (41). Anti-VEGFR-3 blockade or VEGF-C administration did not alter HPSE expression (not shown). To evaluate whether there was a change in HPSE activity, HPSE was inhibited by co-administration into ears of neutralizing anti-HPSE Ab along with anti-VEGFR-3 mAb. Inhibition of HPSE prevented the reduction in HS and dispersion of the CCL21 gradient caused by anti-VEGFR-3 (Fig. 4C and 4D). These results demonstrated that HPSE was constitutively expressed on LEC, HPSE activity was regulated by VEGFR-3, and disruption of HS and the CCL21 gradient around lymphatics was due to HPSE-mediated degradation of HS. Overall, the balance between production and degradation of CCL21 was not directly affected by anti-VEGFR-3 mAb, but rather the loss of the CCL21 gradient was due primarily to the degradation of HS caused by HSPE activity.

The effect of anti-VEGFR-3 is PI3K-dependent

VEGF-C stimulates LEC to up-regulate α4β1 integrin expression via phosphoinositide 3-kinase (PI3K) signaling; and inhibition of PI3K, especially PI3Kα, prevents integrin expression (42). We wondered if PI3Kα signaling also controlled HPSE activity. We characterized the effect of PI3K signaling or blockade with respect to anti-VEGFR-3 treatment. Whole mount IHC showed that a PI3Kα inhibitor, PIK2, decreased expression of CCL21 and HS in the lymphatics, similar to anti-VEGFR-3 mAb. Moreover, a pan-PI3K activator, 740Y-P, prevented anti-VEGFR-3 induced inhibition of CCL21 and HS

expression (Fig. 5A and 5B), indicating that the effects of anti-VEGFR-3 were dependent on PI3K signaling.

CCL21 expression is down-regulated in contact hypersensitivity and dependent on VEGFR-3 down-regulation

To determine the role of VEGFR-3 signaling in the CCL21 gradient in inflammation, we used the DNFB contact hypersensitivity (CHS) model. In positive control ears challenged with DNFB 5 days after sensitization, the expression of VEGFR-3 was down-regulated 48 hours after challenge and LYVE-1 was also down-regulated, as previously reported (43,44) (not shown). CCL21 and HS expression were concurrently down-regulated (not shown). Treating the ears with anti-HPSE or a pan-PI3K activator (740Y-P) 36 hours after DNFB challenge prevented the down-regulation of CCL21 and HS at 48 hours after challenge (Fig. 6). Because of the high fluorescent backgrounds in inflamed ears, we could not reliably quantitate the staining for VEGFR-3, CCL21 or HS; however, the fluorescent images clearly showed marked differences in the distribution and intensity of staining of these molecules, with loss of lymphatic vessel definition as a result of contact sensitization, and regaining lymphatic vessel definition after inhibitor administration. These findings demonstrated that expression of CCL21and HS in inflamed tissues was acutely regulated by VEGFR-3 and dependent on HPSE activity and PI3K signaling.

Discussion

Various roles for VEGFR-3 in lymphatic function have been reported. In acute inflammation, VEGFR-3 stimulation reduces dermal edema by promoting lymph drainage and cell migration (45,46), and regulates lymphangiogenesis and capillary stability (47). Blockade of signaling delays recovery from chronic inflammation (48,49) and exacerbates chronic arthritis (50). VEGF-C/VEGFR-3 signaling maintains tissue electrolyte balance, and signaling blockade leads to tissue accumulation of sodium, chloride, and water (51,52). VEGF-C/VEGFR-3 signaling regulates phasic contractility and diameter of lymphatics in the steady state (53). We showed that VEGFR-3 regulated homeostatic naïve lymphocyte migration by controlling lymphatic HPSE activity, HS scaffold structure, and the CCL21 gradient. Overall, the homeostatic state is not passively regulated, but subject to active receptor and ligand interactions. Future investigations will be needed to dissect out regulation of VEGFR-3 expression and signaling activity.

VEGF-C is constitutively expressed in tissues at a low level (Fig. S2A) in agreement with previous reports (27,54). In addition to fibroblasts and keratinocytes, mononuclear phagocytes also produce VEGF-C, contributing to tissue electrolyte homeostasis and blood pressure control (52). Our results showed that VEGF-C expressed during homeostasis was sufficient to maintain the HS scaffold and CCL21 gradient, and exogenous VEGF-C did not have additional effects on these structures or migration. Although the physiological stimuli for normal VEGF-C production remain to be fully determined, elevated interstitial pressure increases VEGF-C expression in edematous tissues (55). Tonicity-responsive enhancer binding protein in macrophages is activated by high interstitial tonicity and binds the VEGF-C promoter (51). VEGF-C is elevated during acute and chronic inflammation, being

produced by macrophages (46), DC, and neutrophils (56). The complexity of at least five different cell subsets that produce biologically active peptides suggests that there are multiple ways in which homoeostatic and inflammatory responses are engaged to regulate VEGF-C expression and activity and thus lymphatic function.

A CCL21 gradient is formed in tissues (15) and LN (57) to guide migration of $CCR7^+$ leukocytes and for appropriate positioning. CCL21 can be up-regulated (43,44,58) down-regulated (39) or unchanged (38) after various inflammatory events, although the underlying mechanisms are not known. We demonstrated that VEGFR-3 stimulation, PI3Kα activity, HPSE activity, and HS scaffold all influenced the CCL21 gradient. Collagen IV (38) and podoplanin (59) are also involved in immobilization of CCL21 on the abluminal surface of lymphatics and in the interstitium. The turnover of these ECM components should be considered in the regulation of the chemokine gradient. Together these observations show that gradient integrity varies over time and is complex with many possible regulatory cells, molecules, and events.

HPSE is expressed in various cells, including platelets, leukocytes, and BEC (19). We confirmed skin LEC also constitutively expressed HPSE (Fig. 4A and 4B). In the current study, we observed no change in protein expression of HPSE in anti-VEGFR-3 treated tissues, while a neutralizing anti-HPSE Ab inhibited degradation of HS. Therefore, mechanisms other than production or expression of HPSE likely regulated the HS-degrading activity. Additional posttranscriptional mechanisms regulating HPSE activity were reported such as capping on the cell surface (60) and an acidic microenvironment (61,62). HPSE is most active at pH 5.0 (61) and inflamed tissue is known to have a low pH to promote catalytic activity (63,64). Since tissue electrolytes and water homeostasis are regulated by VEGF-C/VEGFR-3 signaling (52), it is possible that VEGFR-3 blockade changed pH leading to HPSE activation in the steady state. Our results also showed that HPSE activity was regulated by VEGFR-3 signaling via PI3Kα during both acute inflammation and homeostasis. Albumin and advance glycated products stimulated HPSE transcription in proximal renal tubular cells and this was also regulated by PI3K (65). These results suggest specific targets for therapeutic regulation of HPSE and hence HS and chemokine gradients.

CHS consists of initiation, persistence and resolution phases. In the persistent inflammation phase, which generally lasts a few days, recruited cells are retained in the tissues as a result of impaired afferent lymph drainage (66). The molecular mechanisms responsible for impaired drainage are poorly understood. Here we observed VEGFR-3 was down-regulated on LEC early after antigenic challenge. Transient down-regulation of VEGFR-3 associated with reduction of the CCL21 gradient is a convincing mechanism leading to cellular, fluid, and molecular retention in inflamed tissues to maximize inflammation. Overexpression of CCL21 impairs cellular retention leading to an attenuated immune response. Indeed, up-regulation of CCL21 prior to hapten challenge promotes $CCR7^+$ cells egress from the skin leading to impaired CHS responses (67). Our data indicated that down-regulation of CCL21 could be reversed by HPSE blockade or PI3K activation, which were down-stream of VEGFR-3 signaling. Taken together, our results demonstrated a novel aspect of VEGF-C/VEGFR-3 signaling in regulating lymphatic function and implicate this signaling as a normal physiologic mechanism in inflammation and as a therapeutic target for treating

persistent inflammation or lymphedema. The definition of roles for CCL21, HS, HPSE, PI3Kα, VEGF-C, and VEGFR-3 points to many opportunities for intervention.

Supplementary Material

Refer to Web version on PubMed Central for supplementary material.

Acknowledgments

We thank Dr. Bronislaw Pytowski, ImClone Systems, for his generous gift of the anti-VEGFR-3 mAb.

Grant Support: NIH R01s AI072039, AI41428, and AI062765; JDRFI 1-2008-90; and the Emerald Foundation (all to JSB).

References

1. Butcher EC, Picker LJ. Lymphocyte Homing and Homeostasis. Science. 1996; 272:60. [PubMed: 8600538]
2. Cose S, Brammer C, Khanna KM, Masopust D, Lefrançois L. Evidence that a significant number of naive T cells enter non-lymphoid organs as part of a normal migratory pathway. European Journal of Immunology. 2006; 36:1423. [PubMed: 16708400]
3. Seabrook T, Au B, Dickstein J, Zhang X, Ristevski B, Hay JB. The traffic of resting lymphocytes through delayed hypersensitivity and chronic inflammatory lesions: a dynamic equilibrium. Seminars in immunology. 1999; 11:115. [PubMed: 10329498]
4. Debes GF, Arnold CN, Young AJ, et al. Chemokine receptor CCR7 required for T lymphocyte exit from peripheral tissues. Nature Immunology. 2005; 6:889. [PubMed: 16116468]
5. Bromley SK, Thomas SY, Luster AD. Chemokine receptor CCR7 guides T cell exit from peripheral tissues and entry into afferent lymphatics. Nature Immunology. 2005; 6:895. [PubMed: 16116469]
6. Förster R, Davalos-Misslitz AC, Rot A. CCR7 and its ligands: balancing immunity and tolerance. Nature Reviews Immunology. 2008; 8:362.
7. Förster R, Schubel A, Breitfeld D, et al. CCR7 coordinates the primary immune response by establishing functional microenvironments in secondary lymphoid organs. Cell. 1999; 99:23. [PubMed: 10520991]
8. Luther SA, Tang HL, Hyman PL, Farr AG, Cyster JG. Coexpression of the chemokines ELC and SLC by T zone stromal cells and deletion of the ELC gene in the plt/plt mouse. Proceedings of the National Academy of Sciences. 2000; 97:12694.
9. Parish CR. The role of heparan sulphate in inflammation. Nature Reviews Immunology. 2006; 6:633.
10. Taylor KR, Gallo RL. Glycosaminoglycans and their proteoglycans: host-associated molecular patterns for initiation and modulation of inflammation. The FASEB Journal. 2006; 20:9.
11. Hirose J, Kawashima H, Swope Willis M, et al. Chondroitin sulfate B exerts its inhibitory effect on secondary lymphoid tissue chemokine (SLC) by binding to the C-terminus of SLC. Biochimica et Biophysica Acta (BBA) - General Subjects. 2002; 1571:219.
12. Schumann K, Lämmermann T, Bruckner M, et al. Immobilized Chemokine Fields and Soluble Chemokine Gradients Cooperatively Shape Migration Patterns of Dendritic Cells. Immunity. 2010; 32:703. [PubMed: 20471289]
13. Bao X, Moseman EA, Saito H, et al. Endothelial Heparan Sulfate Controls Chemokine Presentation in Recruitment of Lymphocytes and Dendritic Cells to Lymph Nodes. Immunity. 2010; 33:817. [PubMed: 21093315]
14. Wang L, Fuster M, Sriramarao P, Esko JD. Endothelial heparan sulfate deficiency impairs L-selectin- and chemokine-mediated neutrophil trafficking during inflammatory responses. Nature immunology. 2005; 6:902. [PubMed: 16056228]

15. Weber M, Hauschild R, Schwarz J, et al. Interstitial dendritic cell guidance by haptotactic chemokine gradients. Science (New York, N Y). 2013; 339:328.
16. Tsuboi K, Hirakawa J, Seki E, et al. Role of high endothelial venule-expressed heparan sulfate in chemokine presentation and lymphocyte homing. Journal of immunology (Baltimore, Md: 1950). 2013; 191:448.
17. McKenzie EA. Heparanase: a target for drug discovery in cancer and inflammation. British Journal of Pharmacology. 2007; 151:1. [PubMed: 17339837]
18. Benhamron S, Nechushtan H, Verbovetski I, et al. Translocation of Active Heparanase to Cell Surface Regulates Degradation of Extracellular Matrix Heparan Sulfate upon Transmigration of Mature Monocyte-Derived Dendritic Cells. The Journal of Immunology. 2006; 176:6417. [PubMed: 16709798]
19. Vlodavsky I, Friedmann Y. Molecular properties and involvement of heparanase in cancer metastasis and angiogenesis. Journal of Clinical Investigation. 2001; 108:341. [PubMed: 11489924]
20. Bartlett MR, Underwood PA, Parish CR. Comparative analysis of the ability of leucocytes, endothelial cells and platelets to degrade the subendothelial basement membrane: evidence for cytokine dependence and detection of a novel sulfatase. Immunology and cell biology. 1995; 73:113. [PubMed: 7797231]
21. Edovitsky E, Lerner I, Zcharia E, Peretz T, Vlodavsky I, Elkin M. Role of endothelial heparanase in delayed-type hypersensitivity. Blood. 2006; 107:3609. [PubMed: 16384929]
22. Hu J, Song X, He YQ, et al. Heparanase and Vascular Endothelial Growth Factor Expression Is Increased in Hypoxia-Induced Retinal Neovascularization. Investigative Ophthalmology & Visual Science. 2012; 53:6810. [PubMed: 22956610]
23. Kaipainen A, Korhonen J, Mustonen T, et al. Expression of the fms-like tyrosine kinase 4 gene becomes restricted to lymphatic endothelium during development. Proceedings of the National Academy of Sciences of the United States of America. 1995; 92:3566. [PubMed: 7724599]
24. Mäkinen T, Norrmén C, Petrova TV. Molecular mechanisms of lymphatic vascular development. Cellular and molecular life sciences: CMLS. 2007; 64:1915. [PubMed: 17458498]
25. Karpanen T, Alitalo K. Molecular biology and pathology of lymphangiogenesis. Annual review of pathology. 2008; 3:367.
26. Shibuya M, Claesson-Welsh L. Signal transduction by VEGF receptors in regulation of angiogenesis and lymphangiogenesis. Experimental cell research. 2006; 312:549. [PubMed: 16336962]
27. Kajiya K, Sawane M, Huggenberger R, Detmar M. Activation of the VEGFR-3 pathway by VEGF-C attenuates UVB-induced edema formation and skin inflammation by promoting lymphangiogenesis. The Journal of investigative dermatology. 2009; 129:1292. [PubMed: 19005491]
28. Trompezinski S, Denis A, Vinche A, Schmitt D, Viac J. IL-4 and interferon-gamma differentially modulate vascular endothelial growth factor release from normal human keratinocytes and fibroblasts. Experimental dermatology. 2002; 11:224. [PubMed: 12102661]
29. Trompezinski S, Berthier-Vergnes O, Denis A, Schmitt D, Viac J. Comparative expression of vascular endothelial growth factor family members, VEGF-B, -C and -D, by normal human keratinocytes and fibroblasts. Experimental dermatology. 2004; 13:98. [PubMed: 15009103]
30. Nykänen AI, Sandelin H, Krebs R, et al. Targeting Lymphatic Vessel Activation and CCL21 Production by Vascular Endothelial Growth Factor Receptor-3 Inhibition Has Novel Immunomodulatory and Antiarteriosclerotic Effects in Cardiac Allografts. Circulation. 2010; 121:1413. [PubMed: 20231530]
31. Chen L, Hamrah P, Cursiefen C, et al. Vascular endothelial growth factor receptor-3 mediates induction of corneal alloimmunity. Nature medicine. 2004; 10:813.
32. Yin N, Zhang N, Lal G, et al. Lymphangiogenesis Is Required for Pancreatic Islet Inflammation and Diabetes. PLoS ONE. 2011; 6:e28023. [PubMed: 22132197]
33. Yin N, Zhang N, Xu J, Shi Q, Ding Y, Bromberg JS. Targeting lymphangiogenesis after islet transplantation prolongs islet allograft survival. Transplantation. 2011; 92:25. [PubMed: 21508896]

34. Issa A, Le TX, Shoushtari AN, Shields JD, Swartz MA. Vascular Endothelial Growth Factor-C and C-C Chemokine Receptor 7 in Tumor Cell–Lymphatic Cross- talk Promote Invasive Phenotype. Cancer Research. 2009; 69:349. [PubMed: 19118020]
35. Pytowski B, Goldman J, Persaud K, et al. Complete and Specific Inhibition of Adult Lymphatic Regeneration by a Novel VEGFR-3 Neutralizing Antibody. Journal of the National Cancer Institute. 2005; 97:14. [PubMed: 15632376]
36. Nakayama Y, Bromberg JS. Lymphotoxin-Beta Receptor Blockade Induces Inflammation and Fibrosis in Tolerized Cardiac Allografts. American Journal of Transplantation. 2012; 12:2322. [PubMed: 22594431]
37. Ledgerwood LG, Lal G, Zhang N, et al. The sphingosine 1-phosphate receptor 1 causes tissue retention by inhibiting the entry of peripheral tissue T lymphocytes into afferent lymphatics. Nature immunology. 2008; 9:42. [PubMed: 18037890]
38. Tal O, Lim HY, Gurevich I, et al. DC mobilization from the skin requires docking to immobilized CCL21 on lymphatic endothelium and intralymphatic crawling. The Journal of Experimental Medicine. 2011; 208:2141. [PubMed: 21930767]
39. Kriehuber E, Breiteneder-Geleff S, Groeger M, et al. Isolation and Characterization of Dermal Lymphatic and Blood Endothelial Cells Reveal Stable and Functionally Specialized Cell Lineages. The Journal of Experimental Medicine. 2001; 194:797. [PubMed: 11560995]
40. Yang BG, Tanaka T, Jang MH, Bai Z, Hayasaka H, Miyasaka M. Binding of Lymphoid Chemokines to Collagen IV That Accumulates in the Basal Lamina of High Endothelial Venules: Its Implications in Lymphocyte Trafficking. The Journal of Immunology. 2007; 179:4376. [PubMed: 17878332]
41. Chen G, Wang D, Vikramadithyan R, et al. Inflammatory cytokines and fatty acids regulate endothelial cell heparanase expression. Biochemistry. 2004; 43:4971. [PubMed: 15109255]
42. Garmy-Susini B, Avraamides CJ, Desgrosellier JS, et al. PI3Kα activates integrin α4β1 to establish a metastatic niche in lymph nodes. Proceedings of the National Academy of Sciences. 2013; 110:9042.
43. Vigl B, Aebischer D, Nitschké M, et al. Tissue inflammation modulates gene expression of lymphatic endothelial cells and dendritic cell migration in a stimulus- dependent manner. Blood. 2011; 118:205. [PubMed: 21596851]
44. Johnson LA, Jackson DG. Inflammation-induced secretion of CCL21 in lymphatic endothelium is a key regulator of integrin-mediated dendritic cell transmigration. International Immunology. 2010; 22:839. [PubMed: 20739459]
45. Huggenberger R, Siddiqui SS, Brander D, et al. An important role of lymphatic vessel activation in limiting acute inflammation. Blood. 2011; 117:4667. [PubMed: 21364190]
46. Kataru RP, Jung K, Jang C, et al. Critical role of CD11b+ macrophages and VEGF in inflammatory lymphangiogenesis, antigen clearance, and inflammation resolution. Blood. 2009; 113:5650. [PubMed: 19346498]
47. Onimaru M, Yonemitsu Y, Fujii T, et al. VEGF-C regulates lymphangiogenesis and capillary stability by regulation of PDGF-B. American journal of physiology Heart and circulatory physiology. 2009; 297:H1685. [PubMed: 19734356]
48. Hagura A, Asai J, Maruyama K, Takenaka H, Kinoshita S, Katoh N. The VEGF- C/VEGFR3 signaling pathway contributes to resolving chronic skin inflammation by activating lymphatic vessel function. Journal of dermatological science. 2014; 73:135. [PubMed: 24252749]
49. Huggenberger R, Ullmann S, Proulx ST, Pytowski B, Alitalo K, Detmar M. Stimulation of lymphangiogenesis via VEGFR-3 inhibits chronic skin inflammation. The Journal of Experimental Medicine. 2010; 207:2255. [PubMed: 20837699]
50. Guo R, Zhou Q, Proulx ST, et al. Inhibition of lymphangiogenesis and lymphatic drainage via vascular endothelial growth factor receptor 3 blockade increases the severity of inflammation in a mouse model of chronic inflammatory arthritis. Arthritis & Rheumatism. 2009; 60:2666. [PubMed: 19714652]
51. Machnik A, Neuhofer W, Jantsch J, et al. Macrophages regulate salt-dependent volume and blood pressure by a vascular endothelial growth factor-C-dependent buffering mechanism. Nature medicine. 2009; 15:545.

52. Wiig H, Schröder A, Neuhofer W, et al. Immune cells control skin lymphatic electrolyte homeostasis and blood pressure. Journal of Clinical Investigation. 2013; 123:2803. [PubMed: 23722907]

53. Breslin JW, Gaudreault N, Watson KD, Reynoso R, Yuan SY, Wu MH. Vascular endothelial growth factor-C stimulates the lymphatic pump by a VEGF receptor-3- dependent mechanism. American Journal of Physiology - Heart and Circulatory Physiology. 2007; 293:H709. [PubMed: 17400713]

54. Uzarski J, Drelles MB, Gibbs SE, et al. The resolution of lymphedema by interstitial flow in the mouse tail skin. American journal of physiology Heart and circulatory physiology. 2008; 294:H1326. [PubMed: 18203849]

55. Rutkowski JM, Moya M, Johannes J, Goldman J, Swartz MA. Secondary lymphedema in the mouse tail: Lymphatic hyperplasia, VEGF-C upregulation, and the protective role of MMP-9. Microvascular Research. 2006; 72:161. [PubMed: 16876204]

56. Baluk P, Tammela T, Ator E, et al. Pathogenesis of persistent lymphatic vessel hyperplasia in chronic airway inflammation. The Journal of clinical investigation. 2005; 115:247. [PubMed: 15668734]

57. Okada T, Miller MJ, Parker I, et al. Antigen-Engaged B Cells Undergo Chemotaxis toward the T Zone and Form Motile Conjugates with Helper T Cells. PLoS Biol. 2005; 3:e150. [PubMed: 15857154]

58. Kish DD, Gorbachev AV, Fairchild RL. IL-1 Receptor Signaling Is Required at Multiple Stages of Sensitization and Elicitation of the Contact Hypersensitivity Response. The Journal of Immunology. 2012; 188:1761. [PubMed: 22238457]

59. Kerjaschki D, Regele HM, Moosberger I, et al. Lymphatic Neoangiogenesis in Human Kidney Transplants Is Associated with Immunologically Active Lymphocytic Infiltrates. Journal of the American Society of Nephrology. 2004; 15:603. [PubMed: 14978162]

60. Sasaki N, Higashi N, Taka T, Nakajima M, Irimura T. Cell Surface Localization of Heparanase on Macrophages Regulates Degradation of Extracellular Matrix Heparan Sulfate. The Journal of Immunology. 2004; 172:3830. [PubMed: 15004189]

61. McKenzie E, Young K, Hircock M, et al. Biochemical characterization of the active heterodimer form of human heparanase (Hpa1) protein expressed in insect cells. Biochemical Journal. 2003; 373:423. [PubMed: 12713442]

62. Ihrcke NS, Parker W, Reissner KJ, Platt JL. Regulation of platelet heparanase during inflammation: role of pH and proteinases. Journal of cellular physiology. 1998; 175:255. [PubMed: 9572470]

63. Wike-Hooley JL, Haveman J, Reinhold HS. The relevance of tumour pH to the treatment of malignant disease. Radiotherapy and oncology: journal of the European Society for Therapeutic Radiology and Oncology. 1984; 2:343. [PubMed: 6097949]

64. Steen KH, Steen AE, Reeh PW. A dominant role of acid pH in inflammatory excitation and sensitization of nociceptors in rat skin, in vitro. The Journal of Neuroscience. 1995; 15:3982. [PubMed: 7751959]

65. Masola V, Gambaro G, Tibaldi E, Onisto M, Abaterusso C, Lupo A. Regulation of heparanase by albumin and advanced glycation end products in proximal tubular cells. Biochimica et biophysica acta. 2011; 1813:1475. [PubMed: 21600934]

66. Liao S, Ruddle NH. Synchrony of High Endothelial Venules and Lymphatic Vessels Revealed by Immunization. The Journal of Immunology. 2006; 177:3369. [PubMed: 16920978]

67. Cummings RJ, Gerber SA, Judge JL, Ryan JL, Pentland AP, Lord EM. Exposure to Ionizing Radiation Induces the Migration of Cutaneous Dendritic Cells by a CCR7- Dependent Mechanism. The Journal of Immunology. 2012; 189:4247. [PubMed: 23002435]

Abbreviations

BEC blood endothelial cells

CHS	contact hypersensitivity
CR	cortical ridge
DNFB	2,4-dinitro-1-fluorobenzene
EC	endothelial cell
ECM	extracellular matrix
HEV	high endothelial venules
HPSE	heparanase
HS	heparan sulfate
IHC	immunohistochemistry
LEC	lymphatic endothelial cells
MS	medullary sinus
SCS	subcapsular sinus
VEGF-C	vascular endothelial growth factor C
VEGFR-3	vascular endothelial growth factor receptor 3

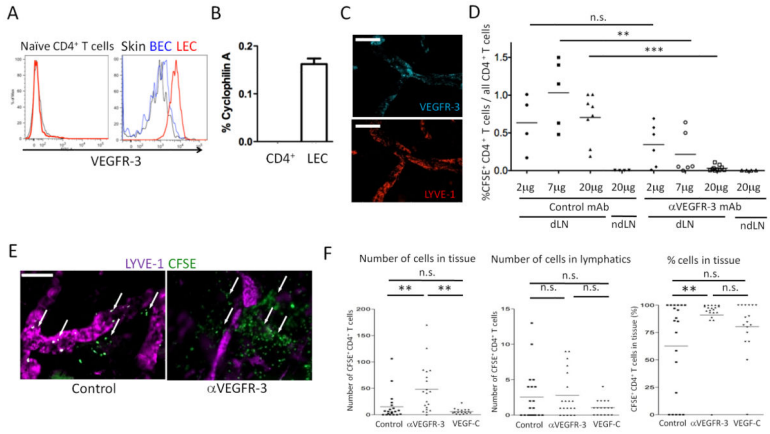

Figure 1. Anti-VEGFR-3 inhibits tissue to lymphatic to dLN migration of CD4$^+$ T cells

(A) VEGFR-3 expression of naïve CD4$^+$ T cells, skin LEC, and skin BEC were analyzed by flow cytometry. Isotype control staining of LEC is shown in black thin solid lines. (B) VEGFR-3 mRNA expression of LEC and naïve CD4$^+$ T cells analyzed by qRT-PCR. The values are shown as relative expression (%) of an endogenous control, cyclophilin A. Results from 2 mice/group, 2 independent experiments. (C) VEGFR-3 expression in afferent lymphatics in skin tissue in whole mount immunohistochemistry. Naive C57BL/6 ear skin sheets stained for LYVE-1 (Cy3) and VEGFR-3 (Cy5). Original magnification 200×. Bars, 100 μm. (D) CFSE-labeled CD4$^+$ T cells plus 2, 7 or 20μg/mouse of control mAb (2A3) or anti-VEGFR-3 mAb (mF4-31C1) injected into foot pads. 12 hours later, popliteal LN (dLN) and axillary LN (ndLN) harvested, percentages of CFSE$^+$ cells in LN CD4$^+$ cells calculated, and compared by one-way ANOVA. Aggregated data are shown. Each point is a foot pad (n = 3-5/group) from 5 independent experiments. ** $p < 0.005$, *** $p < 0.0005$; n.s., not significant. (E) CFSE-labeled CD4$^+$ T cells injected into C57BL/6 ear pinnae with 7μg control or anti-VEGFR-3 mAb, ears harvested at 6 hours, and skin sheets stained for LYVE-1 (Cy5). Representative images with transferred T cells (arrows). Original magnification 200×. Bars, 50 μm. (F) Same as (E), aggregate quantitative data for CFSE$^+$ T cells in tissues and lymphatics at 12 hours. Each point is lymphatics observed in one field, 20 fields/ear from 2 mice/group for 4 independent experiments. ** $p<0.005$; n.s., not significant by one-way ANOVA.

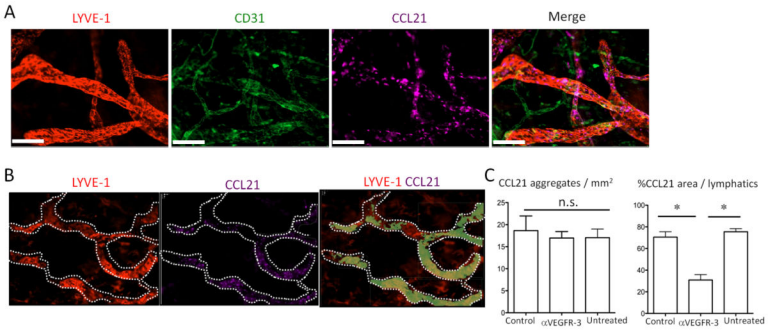

Figure 2. VEGFR-3 regulates CCL21 tissue expression and gradient

(A) Naive ear skin sheets stained for LYVE-1 (Cy3), CD31 (DyeLight 488), and CCL21 (Cy5). Original magnification 200×. Bars, 50 μm. (B) Anti-VEGFR-3 (7μg) or control mAb (7μg) injected into pinnae, ears harvested after 6 hours, and skin sheets stained for LYVE-1 (Cy3) and CCL21 (Cy5). Representative staining pattern of LYVE-1 and CCL21 in lymphatics. CCL21 positive area is shown in light green in the third image. LYVE-1$^+$ lymphatics are traced with white dotted line. (C) Same as (B), CCL21 aggregates (left) or CCL21$^+$ area (right) in lymphatics (at least 10 fields/group) measured. Results from 2 mice/group, 10 independent experiments. * $p<0.05$; n.s., not significant by unpaired *t*-test.

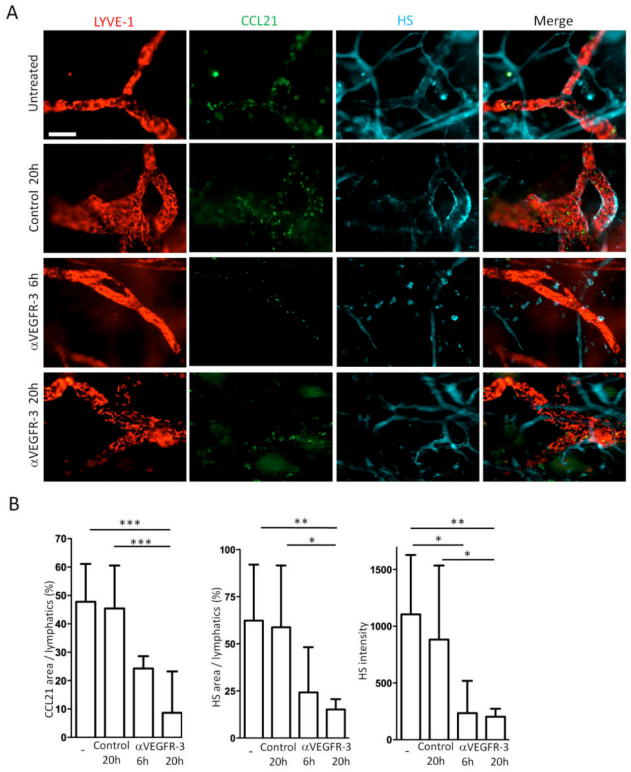

Figure 3. VEGFR-3 regulates heparin sulfate (HS) expression

(A) Anti-VEGFR-3 mAb (7μg) or control mAb (7μg) injected into pinnae, ears harvested 6 or 20 hours later, and skin sheets stained for LYVE-1 (Cy3), CCL21 (Dye Light 488), and HS (Alexa Fluor 647). Original magnification 200×. Bar, 100μm. (B) Same as (A), CCL21 area, HS area, and HS intensity calculated. n = 10-12 fields/group. Results from 2 mice/group, 3 independent experiments. * $p<0.05$, ** $p<0.005$, *** $p<0.0005$ by one-way ANOVA.

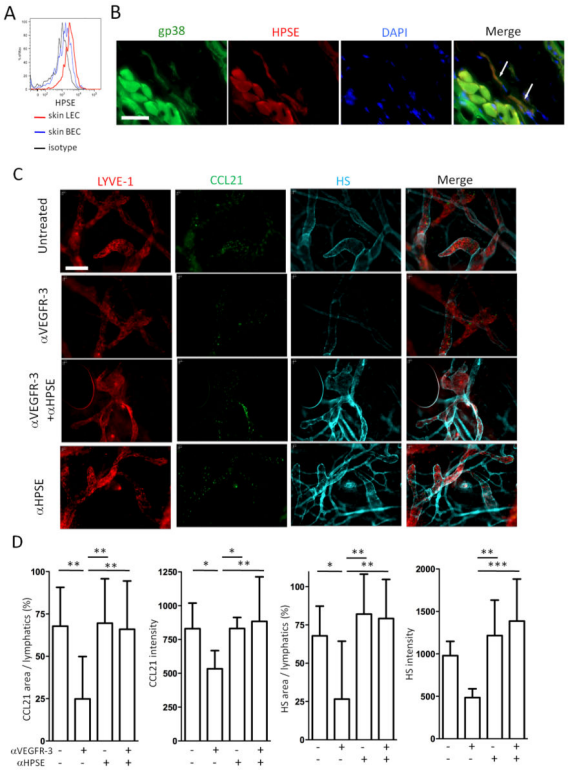

Figure 4. VEGFR-3 regulates HPSE

(A) Ear pinnae single cell suspensions stained for CD45, CD31, gp38, and heparanase (HPSE) and analyzed by flow cytometry. Gating strategy is shown in Fig S1A. HPSE in LEC and BEC are shown. (B) Pinnae stained for HPSE, gp38, and DAPI. Original magnification 600×. Bar, 20μm. White arrows indicate LEC. (C) Control or anti-VEGFR-3 mAb (7μg) injected into pinnae along with anti-HPSE antibody (1μg) intradermally; ears harvested after 20 hours; and stained for LYVE-1 (Cy3), CCL21 (Dye Light 488), and heparan sulfate (HS, Alexa Fluor 647). Original magnification 200×. Bar, 100μm. (D) Same as (C), staining intensity of CCL21 and HS, and %CCL21- and %HS-positive area in lymphatics calculated. n = 10-12 fields/group. Results from 2 mice/group, 3 independent experiments. * $p<0.05$, ** $p<0.005$, *** $p<0.0005$ by one-way ANOVA.

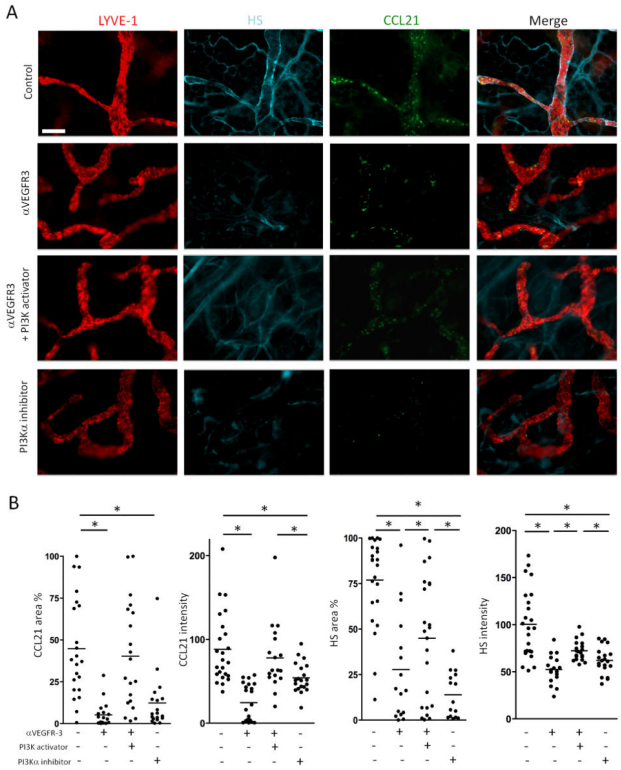

Figure 5. The effects of anti-VEGFR-3 is PI3K dependent

(A) Anti-VEGFR-3 (7μg) or control mAb (7μg) were injected into pinnae with or without PI3Kα inhibitor (PIK2, 10μg) or pan-PI3K activator (740Y-P, 50μg). Six hours later, the ear skin sheets were stained for LYVE-1, CCL21, and HS. Original magnification 200×. Bar, 100μm. (B) Same as (A), staining intensity of CCL21 and HS, and % CCL21- and HS-positive area in LYVE-1+ lymphatics were calculated. n = 10-12 fields/group. Results from 2 mice/group, 3 independent experiments. * $p<0.05$ by one-way ANOVA.

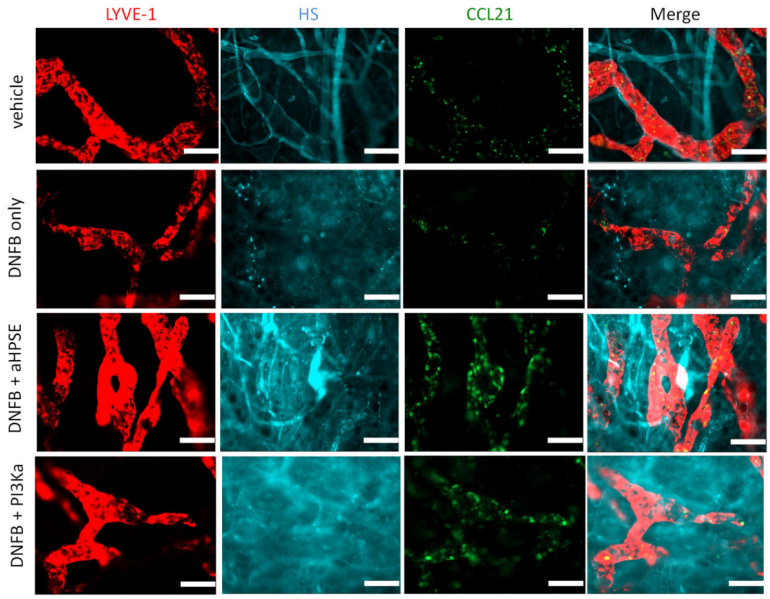

Figure 6. Anti-heparanase and PI3K activator inhibit down-regulation of CCL21 in contact hypersensitivity

Thirty six hours after DNFB challenge or vehicle application, the ears were treated with anti-heparanase Ab (1μg/ear) or PI3K activator (10μg/ear) or PBS. Additional 12 hours later the ear skin sheets were stained for LYVE-1 (Cy3), CCL21 (Dye Light 488), and heparan sulfate (HS, Alexa Fluor 647). Original magnification 200×. Bar, 100μm. Representative images from 2 mice/group, 3 independent experiments.